IEEE Access
Multidisciplinary | Rapid Review | Open Access Journal

Received June 1, 2019, accepted June 18, 2019, date of publication June 24, 2019, date of current version July 15, 2019.

*Digital Object Identifier 10.1109/ACCESS.2019.2924604*

# A Very Deep Densely Connected Network for Compressed Sensing MRI

**KUN ZENG[1,2], YU YANG[1], GUOBAO XIAO[2], AND ZHONG CHEN[1]**

[1]Fujian Provincial Key Laboratory of Plasma and Magnetic Resonance, Department of Electronic Science, School of Electronic Science and Engineering, Xiamen University, Xiamen 361005, China

[2]Fujian Provincial Key Laboratory of Information Processing and Intelligent Control, College of Computer and Control Engineering, Minjiang University, Fuzhou 350108, China

Corresponding author: Zhong Chen (chenz@xmu.edu.cn)

This work was supported in part by the National Science Foundation of China under Grant 61601389, Grant 61601386, and Grant 11761141010.

**ABSTRACT** Convolutional neural network (CNN) has achieved great success in the compressed sensing-based magnetic resonance imaging (CS-MRI). Latest deep networks for CS-MRI usually consist of a stack of sub-networks, each of which refines the former image prediction to a more accurate one. However, as the sub-network number increases, the information in prior sub-networks has a little influence on subsequent ones, which increases the training difficulties and limits the reconstruction performance of the deep model. In this paper, we propose a novel network, named very deep densely connected network (VDDCN), for CS-MRI. Dense connections are introduced to connect any two sub-networks of VDDCN, so each sub-network can make full use of all former predictions, boosting the reconstruction performance of the whole network. The sub-network of VDDCN is composed of feature extraction and fusion block (FEFB) processing data in the image domain and data consistency (DC) layer enforcing the data fidelity in k-space. Specifically, in FEFB, multi-level features are extracted by the recursive feature extraction and fusion sub-blocks (RFEFSBs) and fused locally to obtain the compact features. The VDDCN is much deeper than the prior deep learning models and able to discover more MR image details. The experimental results demonstrate that our proposed VDDCN outperforms other state-of-the-art CS-MRI methods.

**INDEX TERMS** Deep learning, compressed sensing, magnetic resonance imaging (MRI), densely connected network.

## I. INTRODUCTION

Magnetic resonance imaging (MRI) is a non-invasive medical image technique which is widely used in the clinical diagnosis and pathological analysis. However, it takes lots of time for patients to complete a fully-sampled MRI scan. Compressed sensing-based MRI (CS-MRI) is one of the most effective techniques to accelerate magnetic resonance (MR) acquisition, which aims to reconstruct high quality MR images from a small amount of sampling data, instead of fully-sampled data in k-space (i.e. Fourier space).

A number of CS-MRI methods have been proposed in recent years since the CS theory was developed [1], [2]. These methods can be categorized into two groups: model-based methods [3]–[13] and deep learning methods [14]–[29].

The associate editor coordinating the review of this manuscript and approving it for publication was Sudipta Roy.

In model-based methods, CS-MRI is formulated as a penalized inverse problem with the consideration of k-space data fidelity and sparsity in a specific transform domain (e.g. Fourier domain, Discrete cosine transform (DCT) domain [3], wavelet transform domain [4], [5], contourlet transform domain [6]) or an image-adaptive transform domain [7], [8] obtained by dictionary learning methods. In order to improve the quality of the reconstructed images, more data priors are considered, such as total variation penalty [9], [10], local or nonlocal similarity property [11], [12], or low-rank constraint [13]. CS-MRI methods with specific transformation are easy and efficient, but introduce blurring and aliasing artifacts in reconstructed MR image. In contrast, CS-MRI methods with adaptive transformation generally obtain higher quality images, but suffer from slow reconstruction speed.

Recently, deep learning models [14]–[29] have also been adopted to CS-MRI, motivated by the great success

of deep learning in many computer vision applications, such as object recognition [30], [31], image super-resolution [32]–[35], and image segmentation [36]–[38]. Generally, deep learning CS-MRI methods use deep convolutional neural networks (CNNs) to learn the relationship between the under-sampled MRI data and the corresponding fully-sampled MR images in training dataset. With the trained networks, we can obtain the reconstructed MR images from outputs of CNNs, when the given under-sampled MR data are fed to CNNs. Most deep learning CS-MRI methods produce higher quality MR images than model-based CS-MRI algorithms, and the reconstruction procedure is fast because no iterative process is needed. Moreover, the prior information is unnecessary to define explicitly, for it can be learned automatically by deep CNNs [39].

Latest deep learning studies [25]–[29] for CS-MRI focus on learning a deep cascade of multiple sub-networks by introducing data consistency (DC) layer to enforce data fidelity in k-space and improve reconstruction performance. Each sub-network generates a prediction of the reconstructed MR image by using the predicted result of the preceding sub-network. Along the data flow through the network, image predictions are obtained in a 'coarse-to-fine' way. However, these methods could not fully use all former predicted results to predict a new result candidate, thus their image reconstruction performances are limited.

Inspired by densely connected convolutional network (DenseNet) [30], [32], we propose a very deep densely connected network (VDDCN) for CS-MRI. VDDCN makes full use of all former image predictions by combining all sub-networks with dense connections. Each sub-network combines image predictions of all preceding sub-networks, and passes its own prediction to all subsequent sub-networks. Multiple former predictions enable the sub-network to generate an accurate prediction which is useful to reconstruct MR images with high quality. Furthermore, the introduction of dense connections improves the information flowing through the network, alleviating the gradient-vanishing problem and making the network easy to train. The proposed VDDCN is expected to perform better than previous deep learning methods.

The main contributions of this work include the following:

1) We propose a novel deep network VDDCN for CS-MRI. In VDDCN, dense connections are introduced to enable each sub-network to reconstruct a MR image using all previous reconstruction predictions, improving reconstruction performance of the whole network.
2) The sub-networks of VDDCN are specifically designed with residual learning and recursive learning strategies to strengthen their representation power.
3) Extensive experiments show that VDDCN outperforms other state-of-the-art CS-MRI methods in terms of visual results and quantitative evaluations.

The rest of the paper is organized as follows. Section II provides a brief survey of related work. Section III introduces our proposed deep model VDDCN in details. In Section IV, the experimental results and comparisons with several state-of-the-art CS-MRI methods are presented. A summary is given in Section V.

## II. RELATED WORK

Given the vectorized representation $\boldsymbol{x} \in \mathbb{C}^{n^2}$ of a fully-sampled image $\boldsymbol{X} \in \mathbb{C}^{n\times n}$ with size $n \times n$, and its under-sampled k-space measurement $\boldsymbol{y} \in \mathbb{C}^m$ ($m \ll n^2$), the data acquisition model in CS-MRI can be formulated as a discretized linear system as follows:

$$\boldsymbol{y} = \boldsymbol{F}_u\boldsymbol{x} + \boldsymbol{\varepsilon}. \tag{1}$$

Here $\boldsymbol{F}_u = \boldsymbol{U}\boldsymbol{F} \in \mathbb{C}^{m\times n^2}$, in which $\boldsymbol{U} \in \mathbb{C}^{m\times n^2}$ and $\boldsymbol{F} \in \mathbb{C}^{n^2\times n^2}$ are the under-sampling and Fourier transform matrices, and $\boldsymbol{\varepsilon}$ denotes noise. CS-MRI, aiming to recover the underlying $\boldsymbol{x}$ from $\boldsymbol{y}$, is an ill-posed inverse problem.

Generally, model-based CS-MRI methods solve the problem by optimizing

$$\min_{\boldsymbol{x}} \|\boldsymbol{y} - \boldsymbol{F}_u\boldsymbol{x}\|_2^2 + \lambda R(\boldsymbol{x}) \tag{2}$$

where $\|\boldsymbol{y} - \boldsymbol{F}_u\boldsymbol{x}\|_2^2$ is the data fidelity term, $R(\boldsymbol{x})$ denotes the regularization term and the regularization parameter $\lambda$ balances the importance of these two terms.

Different from model-based CS-MRI approaches, deep learning CS-MRI learns a mapping function $\boldsymbol{X} = f(\boldsymbol{X}_0)$ between zero-filling reconstructed image $\boldsymbol{X}_0 \in \mathbb{C}^{n\times n}$ and fully-sampled reconstructed image $\boldsymbol{X}$ by training a CNN with lots of training data. It should be noted that the data fed to CNN are images instead of their vectorized representations. Therefore, $\boldsymbol{X}$ and $\boldsymbol{X}_0$ used in deep learning CS-MRI methods are 2D matrices with size $n \times n$ corresponding to $\boldsymbol{x}$ and $\boldsymbol{F}_u^H\boldsymbol{y}$ respectively, where $(\cdot)^H$ is the conjugated transpose operator.

As the pioneer deep learning model for CS-MRI, a 3-layer CNN was proposed by Wang *et al.* [15] to learn the mapping function in image space between zero-filling reconstructed images and fully-sampled reconstructed images. The same network structure as [15] was employed in [16] to learn the mapping in k-space. Lee *et al.* [17] presented a modified U-net to learn the aliasing artifacts instead of the underlying original image, and Hyun *et al.* [18] showed that the quality of the reconstructed image could be further improved by an additional k-space correction operation. Recently, several generative adversarial nets (GANs) [40] have been introduced to CS-MRI with different generator networks, such as U-net based generator [19] or residual network based generator [20]. In the above mentioned CNNs, no intermediate image prediction is produced, and only a single reconstruction is obtained as the final result.

Meanwhile, various deep networks were introduced for CS-MRI, which generated multiple predicted images with sub-networks and adjusted the predictions to obtain final MR reconstruction with high accuracy. Quan *et al.* [21] proposed RefineGAN in which residual U-net [17] was unfolded

twice to enhance the reconstruction quality. Yang *et al.* [22], [23] presented ADMM-net derived from the iterative procedure of alternating direction method of multipliers (ADMM) algorithm to solve CS-MRI problem. In ADMM-net, Each sub-network corresponds to one iteration of ADMM algorithm. Similar to ADMM-net, variation network proposed by Hammernik *et al.* [24] has several stacked sub-networks related to the steps of Landweber iterative algorithm [41] for CS-MRI. Schlemper *et al.* [25] constructed a deep CS-MRI model by cascading multiple sub-networks and introduced data consistency (DC) layer to correct sub-networks' outputs by considering data fidelity in k-space. Since then, DC layer has become an indispensable component in latest networks [26]–[29] for CS-MRI.

The DC layer updates its input $\widetilde{\boldsymbol{Z}}$ to $\widetilde{\boldsymbol{X}}$ by enforcing data fidelity in k-space between $\widetilde{\boldsymbol{K}} = dft(\widetilde{\boldsymbol{Z}})$ and the original measurement $\boldsymbol{K}_u$, where $dft$ denotes 2D discrete Fourier transformation (DFT) and $\boldsymbol{K}_u$ is a 2D matrix with size $n \times n$ corresponding to $\boldsymbol{U}^H\boldsymbol{y}$. The output function $dc$ of the DC layer can be defined as:

$$\widetilde{\boldsymbol{X}} = dc(\widetilde{\boldsymbol{Z}}, \boldsymbol{K}_u) = idft(\psi(\widetilde{\boldsymbol{K}}, \boldsymbol{K}_u)). \tag{3}$$

Here $idft$ is 2D inverse discrete Fourier transformation (iDFT) and $\psi$ is the data fidelity operation:

$$\psi(\widetilde{\boldsymbol{K}}, \boldsymbol{K}_u)(i,j) = \begin{cases} \widetilde{\boldsymbol{K}}(i,j), & (i,j) \notin \Omega \\ \dfrac{\rho\widetilde{\boldsymbol{K}}(i,j) + \boldsymbol{K}_u(i,j)}{\rho+1}, & (i,j) \in \Omega, \end{cases} \tag{4}$$

where $(i,j)$ is the matrix index, $\Omega$ is the set of sampling positions in k-space and $\rho$ is the noise level. The k-space data in $(i,j)$ that are not sampled in original measurement $\boldsymbol{K}_u$ are evaluated from network prediction $\widetilde{\boldsymbol{K}}(i,j)$, while the k-space data in $(i,j)$ that are sampled in $\boldsymbol{K}_u$ are updated with a linear combination of network prediction $\widetilde{\boldsymbol{K}}(i,j)$ and the original measurement $\boldsymbol{K}_u(i,j)$. In the noiseless case ($\rho = 0$), the data of $\psi(\widetilde{\boldsymbol{K}}, \boldsymbol{K}_u)$ are filled with the original measurement $\boldsymbol{K}_u$ at sampled positions. The function of DC layer is summarized in Figure 1.

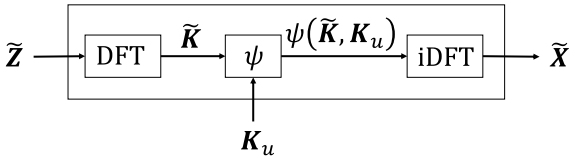


**FIGURE 1.** Function of the DC layer.

However, deep networks [21]–[29] constituted of multiple sub-networks have two major limitations. First, the sub-networks update MR images successively using only the latest prediction, not all the former predictions which might be useful to improve the final reconstruction performance. The second limitation is that most of the networks are too shallow to achieve promising results. To resolve the problems, we propose a very deep network, in which dense connections are used to aggregate all the former predictions to the input of each sub-network.

## III. METHOD

### A. OVERVIEW OF VDDCN

As shown in Figure 2a, our model first produces the zero-filling reconstructed MR image $\boldsymbol{X}_0 = idft(\boldsymbol{K}_u)$ by processing under-sampled k-space data $\boldsymbol{K}_u$ by iDFT, and then generates reconstructed MR image $\hat{\boldsymbol{X}} = f(\boldsymbol{X}_0)$ by a deep network.

The network contains a set of sub-networks, which are connected between each other. As discussed previously, these dense connections enable each sub-network to receive information as much as possible and boost the reconstruction performance of the whole network. Supposing the proposed VDDCN has $K$ sub-networks, the $k$-th ($1 \le k \le K$) sub-network takes all former predictions $\boldsymbol{X}_0, \boldsymbol{X}_1, \cdots, \boldsymbol{X}_{k-1}$ as inputs, and outputs a new prediction $\boldsymbol{X}_k$. So $\boldsymbol{X}_k$ can be formulated by

$$\boldsymbol{X}_k = f_k(\boldsymbol{X}_0, \boldsymbol{X}_1, \cdots, \boldsymbol{X}_{k-1}), \tag{5}$$

where $f_k$ denotes the operation of the $k$-th sub-network, and the final reconstruction result is

$$\hat{\boldsymbol{X}} = f(\boldsymbol{X}_0) = \boldsymbol{X}_K = f_K(\boldsymbol{X}_0, \boldsymbol{X}_1, \cdots, \boldsymbol{X}_{K-1}). \tag{6}$$

Each sub-network consists of one multi-level feature extraction and fusion block (FEFB) and a DC layer. The FEFB generates an intermediate reconstructed image which is updated by the following DC layer. Let us denote the function of FEFB in $k$-th sub-network as $g_k$, the operation $f_k$ of the sub-network includes two steps:

$$\boldsymbol{Z}_k = g_k(\boldsymbol{X}_0, \boldsymbol{X}_1, \cdots, \boldsymbol{X}_{k-1}) \tag{7}$$

and

$$\boldsymbol{X}_k = dc(\boldsymbol{Z}_k, \boldsymbol{K}_u), \tag{8}$$

in which $\boldsymbol{Z}_k$ is the output of the FEFB.

Furthermore, to extract high-level features, complex sub-block named recursive feature extraction and fusion sub-block (RFEFSB) is proposed as the sub-block in FEFB. The structure of FEFB and RFEFSB will be detailed in the following sub-sections.

Because mean absolute error (MAE) has been demonstrated to be more powerful for performance and convergence than mean square error [42], MAE is used in the loss function formulated as

$$L = \frac{1}{N}\sum_{i=1}^{N} \|\hat{\boldsymbol{X}}^{(i)} - \boldsymbol{X}^{(i)}\|_1, \tag{9}$$

where $\boldsymbol{X}^{(i)}$ and $\hat{\boldsymbol{X}}^{(i)}$ are the $i$-th fully-sampled reference image in the training set and the corresponding reconstructed image by our method, and $N$ is the number of training samples.

### B. FEATURE EXTRACTION AND FUSION BLOCK (FEFB)

The structure of FEFB is presented in Figure 2b. Our FEFB contains a Concat+Conv component for shallow feature extraction, several sub-blocks named recursive feature extraction and fusion sub-block (RFEFSB) for multi-level feature

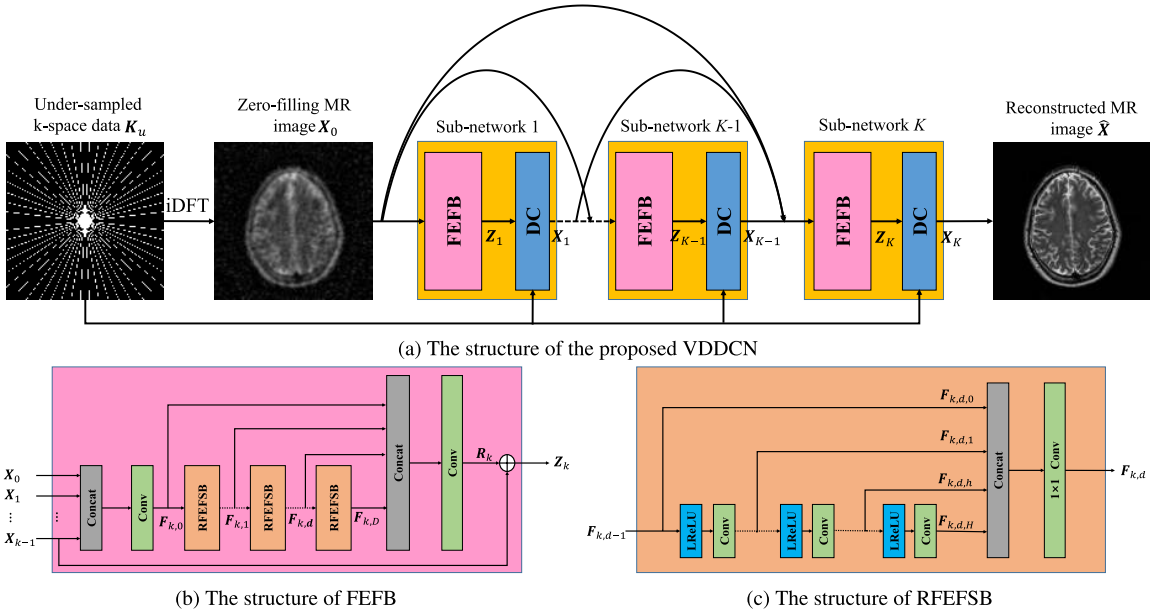


(a) The structure of the proposed VDDCN

(b) The structure of FEFB

(c) The structure of RFEFSB

**FIGURE 2.** **The overview of the proposed VDDCN for CS-MRI.**

extraction, and another Concat+Conv component for feature fusion (FF).

We first concatenate all the inputs and use a convolutional layer to extract shallow features. The shallow features of the FEFB in $k$-th sub-network can be obtained as

$$\boldsymbol{F}_{k,0} = \boldsymbol{W}_k \otimes [\boldsymbol{X}_0, \boldsymbol{X}_1, \cdots, \boldsymbol{X}_{k-1}] + \boldsymbol{b}_k, \tag{10}$$

where $\boldsymbol{W}_k$ is the weight and $\boldsymbol{b}_k$ is the bias of the convolutional layer, and symbol '$\otimes$' denotes the convolution operation. After $\boldsymbol{F}_{k,0}$ is obtained, multi-level features $\boldsymbol{F}_{k,d}$ $(1 \leq d \leq D)$ are generated by multiple RFEFSBs, which are sub-blocks of FEFB:

$$\boldsymbol{F}_{k,d} = \phi_{k,d}(\boldsymbol{F}_{k,d-1}), \tag{11}$$

in which $\phi_{k,d}$ denotes the function of the $d$-th RFEFSB of the FEFB within the $k$-th sub-network. Feature fusion is then applied to fuse all the features $\boldsymbol{F}_{k,d}$ $(0 \leq d \leq D)$, which is described as

$$\boldsymbol{R}_k = \widetilde{\boldsymbol{W}}_k \otimes [\boldsymbol{F}_{k,0}, \boldsymbol{F}_{k,1}, \cdots, \boldsymbol{F}_{k,D}] + \widetilde{\boldsymbol{b}}_k, \tag{12}$$

where $\widetilde{\boldsymbol{W}}_k$ and $\widetilde{\boldsymbol{b}}_k$ are parameters of the convolutional layer in FF part. At last, residual learning [31] is adopted to further improve FEFB's performance. The final output $\boldsymbol{Z}_k$ of the FEFB in the $k$-th sub-network can be obtained by

$$\boldsymbol{Z}_k = \boldsymbol{R}_k + \boldsymbol{X}_{k-1}. \tag{13}$$

### C. RECURSIVE FEATURE EXTRACTION AND FUSION SUB-BLOCK (RFEFSB)

In RFEFSB, leaky rectified linear unit (LReLU) is used as the non-linear activation layer and recursive learning strategy [33], [43] is employed to reduce parameter number. As shown in Figure 2a, a RFEFSB contains $H$ LReLU+Conv components for learning multi-level features recursively and a Concat+Conv component for local feature fusion (LFF). Parameters of LReLU+Conv components are shared within each RFEFSB.

The function of the $h$-th $(1 \leq h \leq H)$ LReLU+Conv component in $d$-th RFEFSB within $k$-th sub-network is

$$\boldsymbol{F}_{k,d,h} = \boldsymbol{W}_{k,d} \otimes \sigma(\boldsymbol{F}_{k,d,h-1}) + \boldsymbol{b}_{k,d}, \tag{14}$$

where $\sigma$ denotes the LReLU activation function, $\boldsymbol{W}_{k,d}$ and $\boldsymbol{b}_{k,d}$ are parameters of the convolutional layer, and $\boldsymbol{F}_{k,d,h}$ is the output of the component. When $h = 1$, $\boldsymbol{F}_{k,d,h-1} = \boldsymbol{F}_{k,d-1}$.

After multi-level features $\boldsymbol{F}_{k,d,h}$ $(0 \leq h \leq H)$ are learned, the LFF part, which has a $1\times1$ convolutional layer, is introduced to generate compact features. The formulation of LFF is written as

$$\boldsymbol{F}_{k,d} = \widetilde{\boldsymbol{W}}_{k,d} \otimes [\boldsymbol{F}_{k,d,0}, \boldsymbol{F}_{k,d,1}, \cdots, \boldsymbol{F}_{k,d,H}] + \widetilde{\boldsymbol{b}}_{k,d}, \tag{15}$$

in which $\widetilde{\boldsymbol{W}}_{k,d}$ is the weight and $\widetilde{\boldsymbol{b}}_{k,d}$ is the bias of the $1\times1$ convolutional layer.

## IV. EXPERIMENTS AND RESULTS

### A. IMPLEMENTATION DETAILS

We use TensorFlow[1] to implement the proposed method on a server installed with an Intel Xeon E5-2620 CPU, a NVIDIA Titan X GPU and 32GB RAM. The network is trained using Adam [44] optimizer for 100 epochs. The learning rate is initialized to 1e-4 and decreases half after 50 epochs. The mini-batch size is set to 1 for all the experiments following the setting of DCCNN [25].

[1] http://www.tensorflow.org/

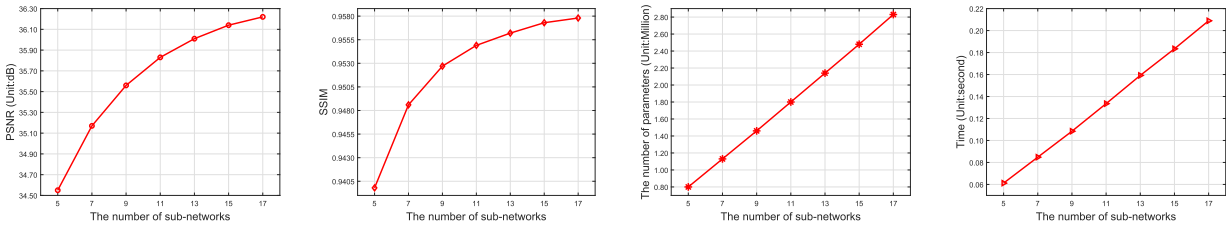


(a) $K$ vs. PSNR (b) $K$ vs. SSIM (c) $K$ vs. parameter number (d) $K$ vs. runing time

**FIGURE 3.** The effects of the sub-network number $K$ in VDDCN on network complexity and performance result.

Two types of commonly used sampling patterns in k-space, including 1D Cartesian under-sampling and pseudo radial under-sampling [9], are studied in this work. The performances of our proposed network are assessed on both real-valued and complex-valued MR images.

The reconstruction results are evaluated with two quality metrics—peak signal-to-noise ratio (PSNR) and structural similarity index measure (SSIM) [45]. We compare our proposed algorithm with four model-based methods (e.g. PANO [11],[2] PBDW [4][2], FDLCP [8][2], BM3D-MRI [12][3]) and two deep learning methods (e.g., U-Net [17], DCCNN [25]).We download source codes for model-based methods from authors' websites, and re-implement these two deep learning methods using TensorFlow.

### B. NETWORK PARAMETERS SELECTION

In our proposed VDDCN, most of the convolutional layers have 64 filters with kernel size of 3×3, except the last convolutional layer of each FEFB, which has 2 filters to produce the real part and the imaginary part of the intermediate reconstructed image.

Besides, there are 3 network parameters in VDDCN, which are the number $D$ of RFEFSBs in each FEFB, the number $H$ of LReLU+Conv components within RFEFSB, and the number $K$ of sub-networks in the whole network. For the sake of simplicity, $D$ and $H$ are set to be 3 empirically and $K$ is determined experimentally.

To select an appropriate $K$, we train and test VDDCN with different sub-network numbers for reconstructing real-valued brain MR images using 10% pseudo radial under-sampling. Figure 3 presents how $K$ affects the network complexity and the reconstruction performance. When $K$ increases from 5 to 17, the PSNR and SSIM increase logarithmically. Meanwhile, the parameter number grows larger and the running time becomes longer in an approximatively linear manner. Specifically, VDDCN with 17 sub-networks obtains little performance improvement (only 0.08dB higher in PSNR and 0.0005 higher in SSIM) compared with VDDCN with 15 sub-networks. To balance between reconstructed image quality and the computational complexity, we select 15 as the default value of $K$.

[2]http://csrc.xmu.edu.cn/

[3]https://web.itu.edu.tr/eksioglue/pubs/BM3D_MRI.htm

### C. REAL-VALUED DATA RECONSTRUCTION

We use brain MR images from the original data acquired from IXI database[4] to assess the performance of our VDDCN to reconstruct real-valued data. 3200 MR images from 80 subjects are normalized and real-valued from the original data, of which 3000 images from 75 subjects are chosen for training, and 200 images from another 5 subjects are for testing. All images are with resolution of 256×256. In addition, sampling rates of 10%, 20%, 30%, and 40%, are tested on both sampling scenarios.

#### 1) IMAGE QUALITY EVALUATION

Figure 4 and 5 show the quantitative results of different methods under different sampling rates using pseudo radial sampling pattern and 1D Cartesian under-sampling pattern, respectively. We can see that, the proposed VDDCN reconstructs the most accurate results compared with other methods under both sampling patterns. Specifically, VDDCN outperforms the second best algorithm DCCNN by at least 2dB.

The visual comparisons of 10% sampling rate on both sampling patterns are shown in Figure 6 and 7. The zero-filling reconstruction is so blurry that few structure details can be observed. The conventional model-based methods, such as PANO, PBDW, FDLCP and BM3D-MRI, produce images with artifacts. U-net gives results that are visually better than model-based methods. DCCNN achieves good performances, but some details are still lost in the reconstructed images. From all the reconstructed images and their corresponding error images, we can see that our proposed VDDCN obtains highest-quality images with finest details and least artifacts.

#### 2) RUNNING TIME EVALUATION

Table 1 presents the average running times of our proposed VDDCN and other CS-MRI methods. It should be noted that all the model-based methods are implemented using MATLAB without GPU-acceleration. For the model-based methods, different iterative numerical algorithms are used and the running times are relatively long. For example, the average running time of PBDW is 94.65 seconds, which is about 500 times as long as the running time of VDDCN. Although PANO is accelerated by adopting parallel

[4]http://brain-development.org/ixi-dataset/

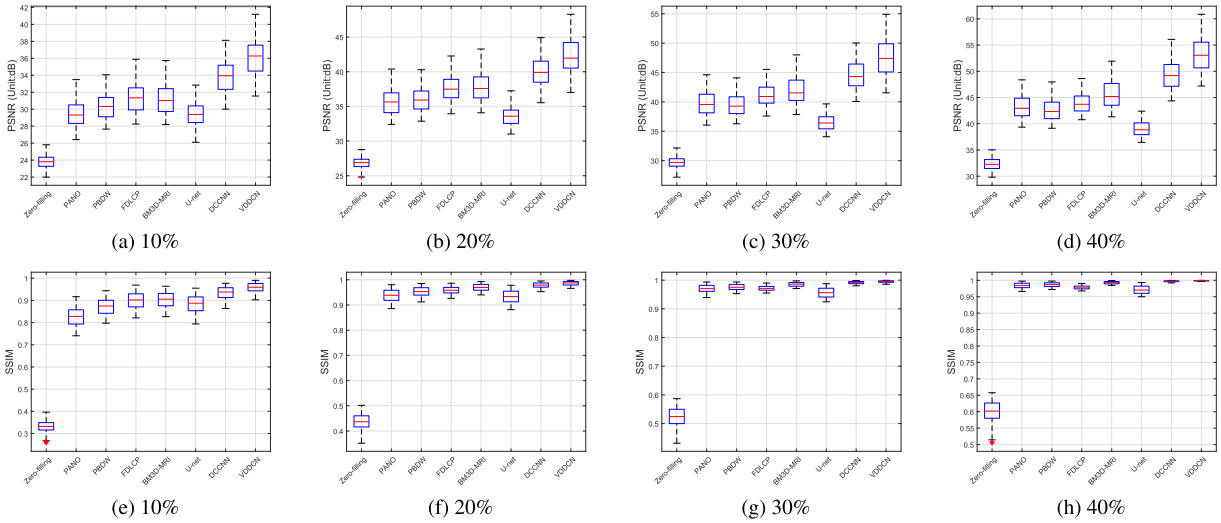


(a) 10% (b) 20% (c) 30% (d) 40%

(e) 10% (f) 20% (g) 30% (h) 40%

**FIGURE 4.** Evaluations on real-valued brain dataset using pseudo radial under-sampling at different sampling rates.

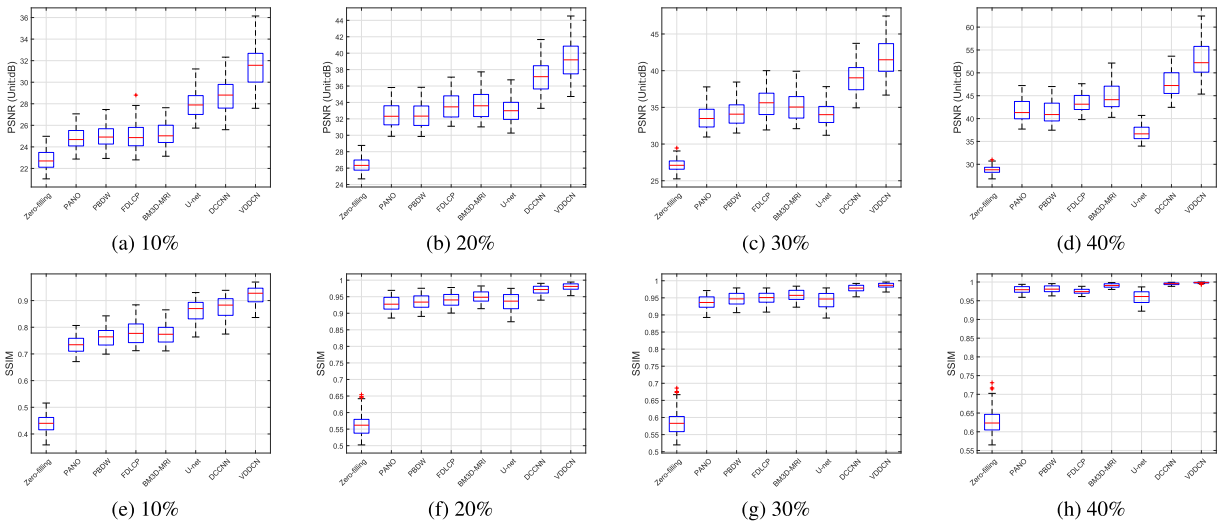


(a) 10% (b) 20% (c) 30% (d) 40%

(e) 10% (f) 20% (g) 30% (h) 40%

**FIGURE 5.** Evaluations on real-valued brain dataset using 1D Cartesian under-sampling at different sampling rates.

**TABLE 1.** Running time comparison of CS-MRI methods on real-valued brain images using 10% pseudo radial under-sampling.

| Method | PANO [11] | PBDW [4] | FDLCP [8] | BM3D-MRI [12] | U-net [17] | DCCNN [25] | VDDCN |
|---|---|---|---|---|---|---|---|
| Time (Unit:second) | 9.02 | 94.65 | 72.27 | 12.63 | 0.02 | 0.02 | 0.18 |

computing strategy, its running time is still far from interactive (around 9 seconds).

Deep learning based methods, including U-net, DCCNN, and VDDCN, run much faster than model-based methods, because that these deep learning based methods employ feed-forward CNNs and use GPU to accelerate the image reconstruction procedure. The running times of U-net and DCCNN are about 0.02 second, which can meet the requirement of real-time implementation. Compared with U-net and DCCNN, VDDCN takes more time (i.e. 0.18 second) to complete image reconstruction since VDDCN is a much deeper network with more complex structure. However, the additional time cost of VDDCN is acceptable considering its performance improvement.

### D. COMPLEX-VALUED DATA RECONSTRUCTION

We further investigate the performance of our proposed VDDCN for reconstructing complex-valued knee images.[5] The dataset contains 200 images with resolution of 256×256. We choose 150 images for training and the rest for testing. The experiments are conducted in sampling rate of 10% under pseudo radial sampling pattern and 1D Cartesian under-sampling pattern. The quantitative evaluation results are shown in Figure 8. It can be seen that our VDDCN outperforms the compared CS-MRI methods. Figure 9 illustrates the reconstructed magnitude and phase images under 1D Cartesian under-sampling. The four model-based

[5]http://old.mridata.org/fullysampled/knees

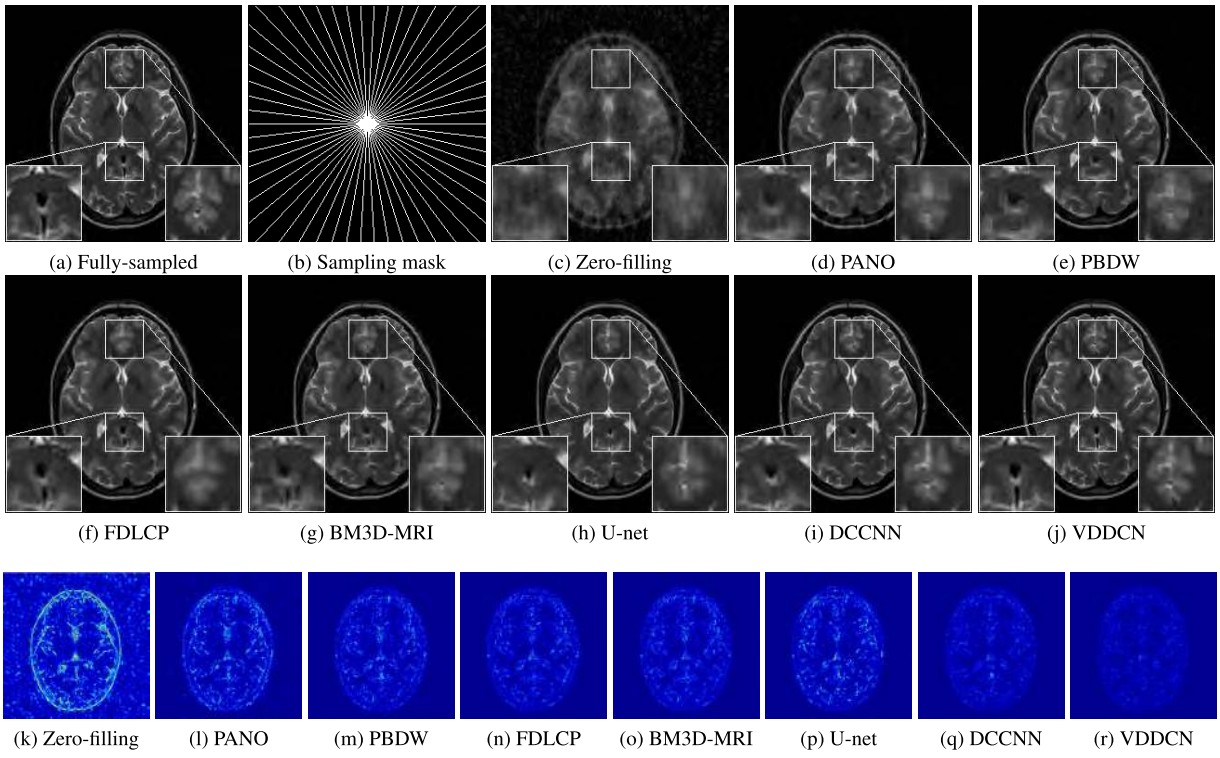


**FIGURE 6.** Results on a brain MR image using 10% pseudo radial under-sampling. The colorbar range of error images is [0, 0.60].

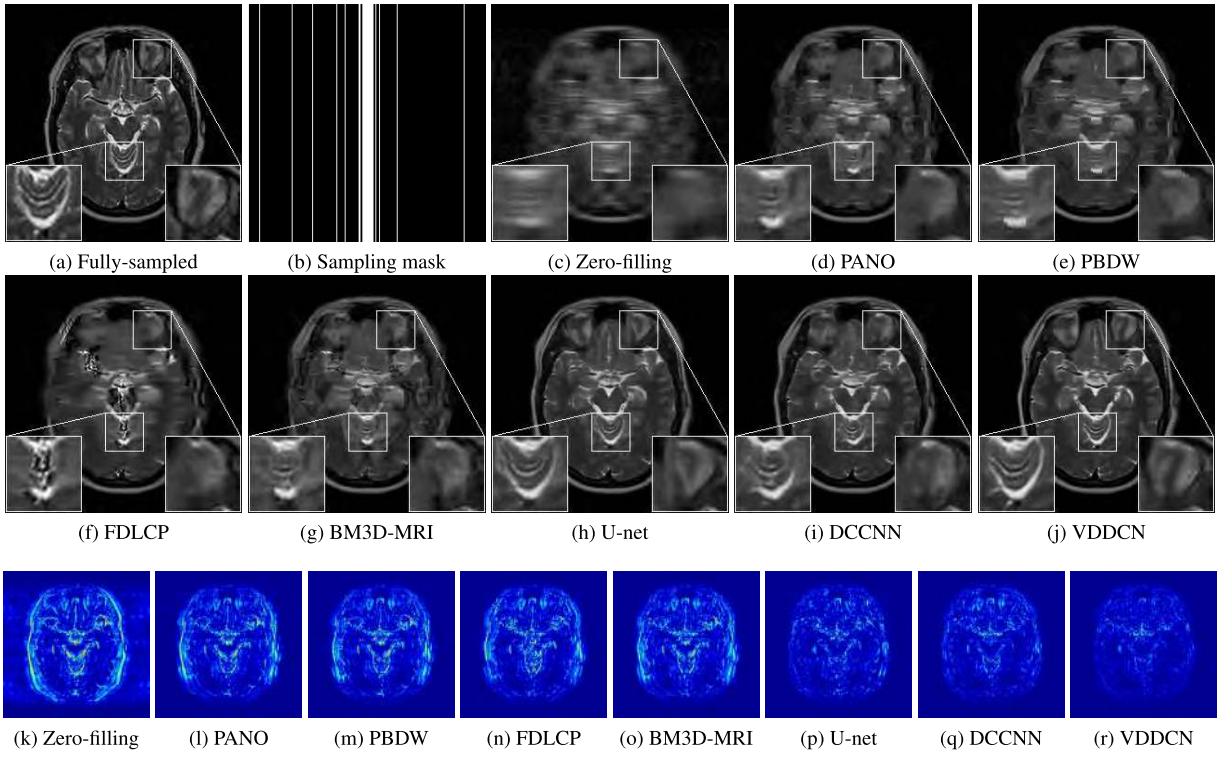


**FIGURE 7.** Results on a brain MR image using 10% 1D Cartesian under-sampling. The colorbar range of error images is [0, 0.45].

methods fail to obtain convincing reconstructions, while deep learning methods gain better results than model-based methods. Compared with DCCNN, U-net reconstructs magnitude image with more artifacts. However, U-net discovers more fine details in phase image. VDDCN achieves least error in magnitude image, and preserves sharpest edges in phase image. Both of the magnitude and phase images reconstructed by VDDCN are most similar to the ground truths.

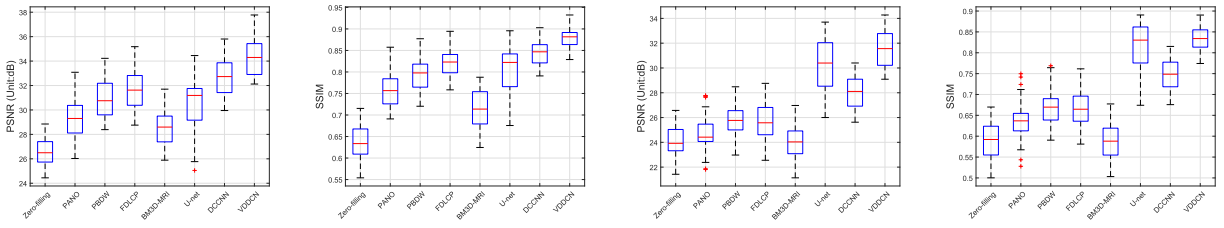


**FIGURE 8.** Evaluations on complex-valued knee dataset under two sampling patterns at 10% sampling rate. (a) and (b) are tested under pseudo radial under-sampling pattern, while (c) and (d) are tested under 1D Cartesian under-sampling pattern.

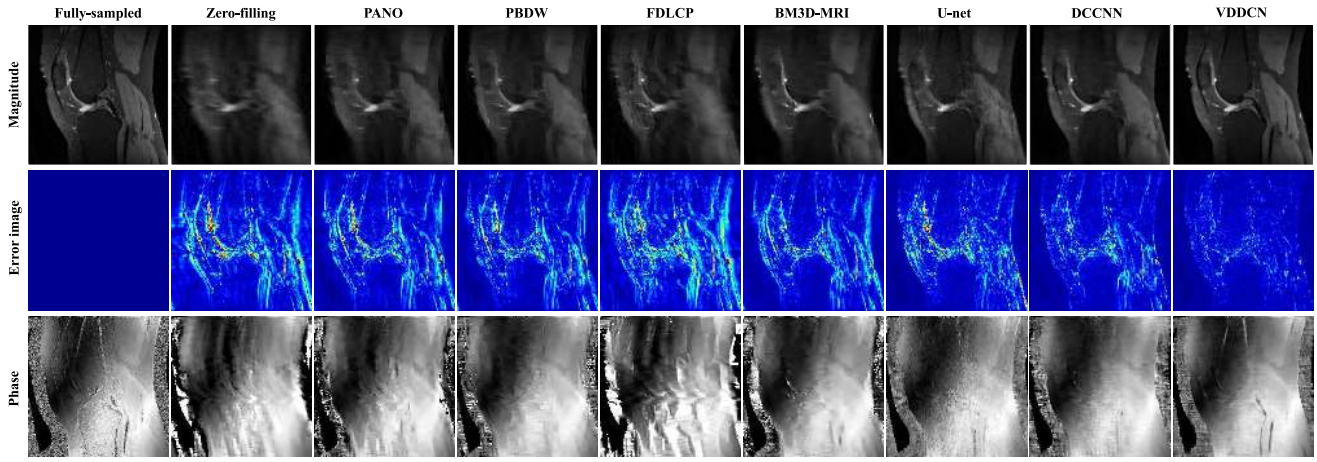


**FIGURE 9.** Results on a knee MR image using 10% 1D Cartesian under-sampling. The colorbar range of error images is [0, 0.25].

## V. CONCLUSION

In this paper, we introduce a novel deep learning model, named very deep densely connected network (VDDCN), for CS-MRI. The proposed VDDCN is composed of several sub-networks, each of which consists of a feature extraction and fusion block (FEFB) processing data in image domain and a data consistency layer enforcing the data fidelity in k-space. Dense connections between the sub-networks are employed to improve the reconstruction performance for CS-MRI. The FEFB in each sub-network is constituted of several sub-blocks named recursive feature extraction and fusion sub-block (RFEFSB). FEFB and its sub-blocks are specifically designed with a combination of the effective structures of residual CNN and recursive CNN. The proposed VDDCN is tested under pseudo radial sampling pattern and 1D Cartesian under-sampling pattern. Extensive experiments demonstrate that the proposed VDDCN outperforms other state-of-the-art methods with visually and quantitatively superior results. For the future work, we will explore use of VDDCN for parallel magnetic resonance imaging (pMRI) and CS-pMRI.

## REFERENCES

[1] E. J. Candès, J. Romberg, and T. Tao, "Robust uncertainty principles: Exact signal reconstruction from highly incomplete frequency information," *IEEE Trans. Inf. Theory*, vol. 52, no. 2, pp. 489–509, Feb. 2006.

[2] D. L. Donoho, "Compressed sensing," *IEEE Trans. Inf. Theory*, vol. 52, no. 4, pp. 1289–1306, Apr. 2006.

[3] M. Lustig, D. Donoho, and J. M. Pauly, "Sparse MRI: The application of compressed sensing for rapid MR imaging," *Magn. Reson. Med.*, vol. 58, no. 6, pp. 1182–1195, 2007.

[4] X. Qu, D. Guo, B. Ning, Y. Lin, S. Cai, and Z. Chen, "Undersampled MRI reconstruction with patch-based directional wavelets," *Magn. Reson. Imag.*, vol. 30, no. 7, pp. 964–977, Sep. 2012.

[5] R. W. Liu, Q. Ma, S. C. H. Yu, K. T. Chui, and N. Xiong, "Variational regularized tree-structured wavelet sparsity for CS-SENSE parallel imaging," *IEEE Access*, vol. 6, pp. 61050–61064, 2018.

[6] S.-M. Gho, Y. Nam, S.-Y. Zho, E. Y. Kim, and D.-H. Kim, "Three dimension double inversion recovery gray matter imaging using compressed sensing," *Magn. Reson. Imag.*, vol. 28, no. 10, pp. 1395–1402, 2010.

[7] S. Ravishankar and Y. Bresler, "MR image reconstruction from highly undersampled k-space data by dictionary learning," *IEEE Trans. Med. Imag.*, vol. 30, no. 5, pp. 1028–1041, May 2011.

[8] Z. Zhan, J.-F. Cai, D. Guo, Y. Liu, Z. Chen, and X. Qu, "Fast multiclass dictionaries learning with geometrical directions in MRI reconstruction," *IEEE Trans. Biomed. Eng.*, vol. 63, no. 9, pp. 1850–1861, Sep. 2016.

[9] K. T. Block, M. Uecker, and J. Frahm, "Undersampled radial MRI with multiple coils. Iterative image reconstruction using a total variation constraint," *Magn. Reson. Med.*, vol. 57, no. 6, pp. 1086–1098, 2007.

[10] X. Fan, Q. Lian, and B. Shi, "Compressed sensing MRI with phase noise disturbance based on adaptive tight frame and total variation," *IEEE Access*, vol. 5, pp. 19311–19321, 2017.

[11] X. Qu, Y. Hou, F. Lam, D. Guo, J. Zhong, and Z. Chen, "Magnetic resonance image reconstruction from undersampled measurements using a patch-based nonlocal operator," *Med. Image Anal.*, vol. 18, pp. 843–856, Aug. 2014.

[12] E. M. Eksioglu, "Decoupled algorithm for MRI reconstruction using nonlocal block matching model: BM3D-MRI," *J. Math. Imag. Vis.*, vol. 56, no. 3, pp. 430–440, 2016.

[13] B. Trémoulheac, N. Dikaios, D. Atkinson, and S. R. Arridge, "Dynamic MR image reconstruction–separation from undersampled $(k, t)$-space via low-rank plus sparse prior," *IEEE Trans. Med. Imag.*, vol. 33, no. 8, pp. 1689–1701, Aug. 2014.

[14] B. Zhu, J. Z. Liu, S. F. Cauley, B. R. Rosen, and M. S. Rosen, "Image reconstruction by domain-transform manifold learning," *Nature*, vol. 555, pp. 487–492, Mar. 2018.

[15] S. Wang, Z. Su, L. Ying, X. Peng, S. Zhu, F. Liang, D. Feng, and D. Liang, "Accelerating magnetic resonance imaging via deep learning," in *Proc. IEEE Int. Symp. Biomed. Imag.*, Apr. 2016, pp. 514–517.

[16] M. Akçakaya, S. Moeller, S. Weingärtner, and K. Uğurbil, "Scan-specific robust artificial-neural-networks for k-space interpolation (RAKI) reconstruction: Database-free deep learning for fast imaging," *Magn. Reson. Med.*, vol. 81, no. 1, pp. 439–453, 2019.

[17] D. Lee, J. Yoo, and J. C. Ye, "Deep residual learning for compressed sensing MRI," in *Proc. IEEE Int. Symp. Biomed. Imag.*, Apr. 2017, pp. 15–18.

[18] C. M. Hyun, H. P. Kim, S. M. Lee, S. Lee, and J. K. Seo, "Deep learning for undersampled MRI reconstruction," *Phys. Med. Biol.*, vol. 63, no. 13, pp. 135007:1–135007:15, 2018.

[19] G. Yang, S. Yu, H. Dong, G. Slabaugh, P. L. Dragotti, X. Ye, F. Liu, S. Arridge, J. Keegan, Y. Guo, and D. Firmin, "DAGAN: Deep de-aliasing generative adversarial networks for fast compressed sensing MRI reconstruction," *IEEE Trans. Med. Imag.*, vol. 37, no. 6, pp. 1310–1321, Jun. 2018.

[20] M. Mardani, E. Gong, J. Y. Cheng, S. S. Vasanawala, G. Zaharchuk, L. Xing, and J. M. Pauly, "Deep generative adversarial neural Networks for compressive sensing MRI," *IEEE Trans. Med. Imag.*, vol. 38, no. 1, pp. 167–179, Jan. 2019.

[21] T. M. Quan, T. Nguyen-Duc, and W.-K. Jeong, "Compressed sensing MRI reconstruction using a generative adversarial network with a cyclic loss," *IEEE Trans. Med. Imag.*, vol. 37, no. 6, pp. 1488–1497, Jun. 2018.

[22] Y. Yang, J. Sun, H. Li, and Z. Xu, "Deep ADMM-net for compressive sensing MRI," in *Proc. Adv. Neural Inf. Process. Syst.*, 2016, pp. 10–18.

[23] Y. Yang, J. Sun, H. Li, and Z. Xu, "ADMM-CSNet: A deep learning approach for image compressive sensing," *IEEE Trans. Pattern Anal. Mach. Intell.*, to be published. doi: 10.1109/TPAMI.2018.2883941.

[24] K. Hammernik, T. Klatzer, E. Kobler, M. P. Recht, D. K. Sodickson, T. Pock, and F. Knoll, "Learning a variational network for reconstruction of accelerated MRI data," *Magn. Reson. Med.*, vol. 79, no. 6, pp. 3055–3071, 2017.

[25] J. Schlemper, J. Caballero, J. V. Hajnal, A. N. Price, and D. Rueckert, "A deep cascade of convolutional neural networks for dynamic mr image reconstruction," *IEEE Trans. Med. Imag.*, vol. 37, no. 2, pp. 491–503, Feb. 2017.

[26] T. Eo, Y. Jun, T. Kim, J. Jang, H.-J. Lee, and D. Hwang, "KIKI-net: Cross-domain convolutional neural networks for reconstructing undersampled magnetic resonance images," *Magn. Reson. Med.*, vol. 80, no. 5, pp. 2188–2201, 2018.

[27] L. Sun, Z. Fan, Y. Huang, X. Ding, and J. Paisley, "Compressed sensing MRI using a recursive dilated network," in *Proc. 32nd AAAI Conf. Artif. Intell.*, 2018, pp. 2444–2451.

[28] Z. Fan, L. Sun, X. Ding, Y. Huang, C. Cai, and J. Paisley, "A segmentation-aware deep fusion network for compressed sensing MRI," in *Proc. Eur. Conf. Comput. Vis.*, 2018, pp. 55–70.

[29] Q. Huang, D. Yang, P. Wu, H. Qi, J. Yi, and D. Metaxas, "MRI reconstruction via cascaded channel-wise attention network," in *Proc. IEEE Int. Symp. Biomed. Imag.*, Apr. 2019, pp. 1622–1626.

[30] G. Huang, Z. Liu, L. van der Maaten, and K. Q. Weinberger, "Densely connected convolutional networks," in *Proc. IEEE Conf. Comput. Vis. Pattern Recognit.*, Jul. 2017, pp. 2261–2269.

[31] K. He, X. Zhang, S. Ren, and J. Sun, "Deep residual learning for image recognition," in *Proc. IEEE Conf. Comput. Vis. Pattern Recognit.*, Jun. 2016, pp. 770–778.

[32] T. Tong, G. Li, X. Liu, and Q. Gao, "Image super-resolution using dense skip connections," in *Proc. IEEE Int. Conf. Comput. Vis.*, Oct. 2017, pp. 4809–4817.

[33] J. Kim, J. Lee, and K. M. Lee, "Deeply-recursive convolutional network for image super-resolution," in *Proc. IEEE Conf. Comput. Vis. Pattern Recognit.*, Jun. 2016, pp. 1637–1645.

[34] K. Zeng, J. Yu, R. Wang, C. Li, and D. Tao, "Coupled deep autoencoder for single image super-resolution," *IEEE Trans. Cybern.*, vol. 47, no. 1, pp. 27–37, Jan. 2017.

[35] Y. Li, B. Song, J. Guo, X. Du, and M. Guizani, "Super-resolution of brain MRI images using overcomplete dictionaries and nonlocal similarity," *IEEE Access*, vol. 7, pp. 25897–25907, 2019.

[36] Q. Zhu, B. Du, P. Yan, H. Lu, and L. Zhang, "Shape prior constrained PSO model for bladder wall MRI segmentation," *Neurocomputing*, vol. 294, pp. 19–28, Jun. 2017.

[37] Q. Zhu, B. Du, B. Turkbey, P. Choyke, and P. Yan, "Exploiting interslice correlation for MRI prostate image segmentation, from recursive neural networks aspect," *Complexity*, vol. 2018, Feb. 2018, Art. no. 4185279.

[38] O. Ronneberger, P. Fischer, and T. Brox, "U-net: Convolutional networks for biomedical image segmentation," in *Proc. Int. Conf. Med. Image Comput. Comput.-Assist. Intervent.*, 2015, pp. 234–241.

[39] B. Du, W. Xiong, J. Wu, L. Zhang, L. Zhang, and D. Tao, "Stacked convolutional denoising auto-encoders for feature representation," *IEEE Trans. Cybern.*, vol. 47, no. 4, pp. 1017–1027, Apr. 2017.

[40] I. Goodfellow, J. Pouget-Abadie, M. Mirza, B. Xu, D. Warde-Farley, S. Ozair, A. Courville, and Y. Bengio, "Generative adversarial nets," in *Proc. Adv. Neural Inf. Process. Syst.*, 2014, pp. 2672–2680.

[41] L. Landweber, "An iteration formula for fredholm integral equations of the first kind," *Amer. J. Math.*, vol. 73, no. 3, pp. 615–624, Jul. 1951.

[42] H. Zhao, O. Gallo, I. Frosio, and J. Kautz, "Loss functions for image restoration with neural networks," *IEEE Trans. Comput. Imag.*, vol. 3, no. 1, pp. 47–57, Mar. 2017.

[43] R. Socher, B. Huval, B. Bhat, C. D. Manning, and A. Y. Ng, "Convolutional-recursive deep learning for 3D object classification," in *Proc. Adv. Neural Inf. Process. Syst.*, 2012, pp. 656–664.

[44] D. Kingma and J. Ba, "Adam: A method for stochastic optimization," in *Proc. 3rd Int. Conf. Learn. Represent.*, 2015, pp. 1–15.

[45] Z. Wang, A. C. Bovik, H. R. Sheikh, and E. P. Simoncelli, "Image quality assessment: From error visibility to structural similarity," *IEEE Trans. Image Process.*, vol. 13, no. 4, pp. 600–612, Apr. 2004.

**KUN ZENG** received the B.Eng., M.Sc., and Ph. D degrees from the Department of Computer Science, Xiamen University, Xiamen, China, in 2005, 2008, and 2015, respectively, where he currently holds a postdoctoral position with the Department of Electronic Science. His current research interests include image processing, machine learning, and medical image reconstruction.

**YU YANG** received the B.S. degree in acoustics from Nanjing University, China, in 2004, and the Ph.D. degree in electrical engineering from Tsinghua University, Beijing, China, in 2009. Since 2015, she has been an Assistant Professor with the Electronic Science Department, Xiamen University, Xiamen, China. Her research interests include magnetic resonance, signal processing, and evolutionary algorithms.

**GUOBAO XIAO** received the Ph.D. degree in computer science and technology from Xiamen University, China, in 2016, where he was a Post-doctoral Fellow with the School of Aerospace Engineering, from 2016 to 2018. He is currently a Professor with Minjiang University, China. He has published over 30 papers in the international journals and conferences, including the IEEE TRANSACTIONS ON PATTERN ANALYSIS and *Machine Intelligence*, *International Journal of Computer Vision*, *Pattern Recognition*, *Pattern Recognition Letters*, *Computer Vision and Image Understanding*, ICCV, ECCV, ACCV, AAAI, ICIP, and ICARCV. His research interests include machine learning, computer vision, pattern recognition, and bioinformatics. He was awarded the Best Ph.D. Thesis in Fujian Province and the Best Ph.D. Thesis Award by the China Society of Image and Graphics. He serves on the reviewer panel for some international journals and top conferences.

**ZHONG CHEN** received the Ph.D. degree from Xiamen University, China, in 1993. In 1995, he joined Xiamen University as an Associate Professor and was appointed as the Director of the Magnetic Resonance Center. From 1998 to 2000, he was a Visiting Associate Professor with the University of Rochester, USA, where he has been a Full Professor with the Department of Physics/Electronic Science, since 2000. His research interest includes nuclear magnetic resonance techniques and applications.